

Flat lens without optical axis: Theory of imaging

W. T. Lu* and S. Sridhar†

Department of Physics and Electronic Materials Research Institute, Northeastern University, Boston, MA 02115

(Dated: October 26, 2018)

We derive a general theory for imaging by a flat lens without optical axis. We show that the condition for imaging requires a material having *elliptic dispersion relations with negative group refraction*. This medium is characterized by two intrinsic parameters σ and κ . Imaging can be achieved with both negative and positive wave vector refraction if σ is a positive constant. The Veselago-Pendry lens is a special case with $\sigma = 1$ and $\kappa = 0$. A general law of refraction for anisotropic media is revealed. Realizations of the imaging conditions using anisotropic media and inhomogeneous media, particularly photonic crystals, are discussed. Numerical examples of imaging and requirements for sub-wavelength imaging are also presented.

PACS numbers: 78.20.Ci, 42.70.Qs, 42.30.Wb

Since antiquity, the positive index of refraction of conventional materials has required the use of curved surfaces to focus light. However there has been a continuing quest for lenses with flat surfaces as they confer a variety of advantages. Notable examples are the Fresnel lens and Maxwell's fish eye lens [1, 2]. The Fresnel flat lens uses a gradient-index $n(x)$ material (GRIN) [3, 4, 5] and hence must possess an optical axis, i.e. is not translationally invariant along the surface (x -axis).

The concept of negative refraction has led to new fundamental approaches as well as applications in optics [6]. In 1968 Veselago [7] pointed out that for a material with refractive index $n = -1$ a flat surface would focus light. A decade later, Silin [8] discussed a more general case and obtained the lens equation of a flat slab with negative elliptic dispersion. Pendry's recent analysis [9] demonstrating the possibility of sub-wavelength resolution with a flat slab of such materials, as well as the experimental realization of the so-called left-handed materials using composite media [10] and photonic crystals (PhCs) [11, 12] led to renewed interest in the unique electromagnetic properties of these artificial materials. The unique property of these flat lenses is the lack of optical axis. This type of flat lenses can be realized in a PhC using negative refraction [13] and has been demonstrated in microwave experiment [14]. Super-resolution imaging through single negative index media are also studied [15, 16, 17, 18]. There is however no complete theory of imaging by a flat lens which properly describes the various features observed in the experiments and in numerical simulations.

In this paper, we present a general theory of imaging by a flat lens without optical axis, resulting in a proposal for a new material which is translationally invariant along the surface and has anisotropic refractive index $n(\theta)$. Defining an optical phase condition for imaging, we show that the condition requires a material having *Ellip-*

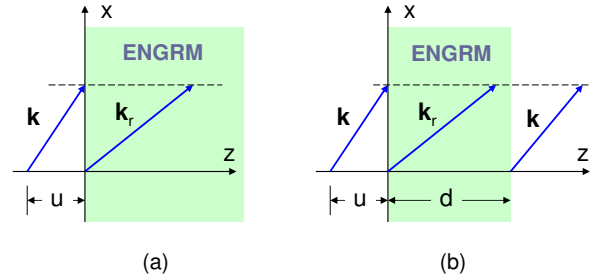


FIG. 1: Wave vector refraction for (a) a single interface between the vacuum and an ENGRM and (b) an ENGRM slab.

tic dispersion relations with Negative Group Refraction (ENGRM) at the operating frequency. The ENGRM is defined by two parameters: the anisotropy parameter σ which is a measure of the ellipse eccentricity, and a phase factor κ which determines the center of the ellipse. Refraction laws for the wave vector and the group velocity for anisotropic media are derived. The theory shows that “perfect” images can be obtained, and *imaging is possible with negative as well positive refractive indices*. The required conditions and consequences of flat perfect and imperfect lenses made of ENGRMs are derived from a generalized Fermat's principle. Realization of flat lenses using PhCs is discussed. In real PhCs, σ is itself angle-dependent in most cases, leading to some limitations for image formation. Many of the proposals for PhC lenses are contained in the present theory. The theory is also applied to recent experiments using PhCs and is shown to successfully describe some intriguing aspects of the data. Numerical simulations are presented that describe visual details of the image formation in PhCs.

We first consider the case of a single interface which is along the x -axis and at $z = 0$ as shown in Fig. 1(a). The wave vector \mathbf{k} of an incident plane wave from vacuum towards the interface makes an angle θ with the z -axis. Here we consider the case that for any incident \mathbf{k} , there is only one refractive wave vector \mathbf{k}_r . Continuity along the interface requires that $k_{rx} = k_x$. A point source is at $x = 0$ and $z = -u$ with $u > 0$. We now consider

*Electronic address: w.lu@neu.edu

†Electronic address: s.sridhar@neu.edu

another point in the ENGRM at $x = \Delta x$ and $z = v$ with $v > 0$. The phase difference between these two points for each incident \mathbf{k} is $\Phi = \Phi_z + \Phi_x$ with $\Phi_z = k_z u + k_{rz} v$ and $\Phi_x = k_x \Delta x$. According to Fermat's principle, the formation of an image would require that the total phase Φ be stationary. This restriction can be relaxed for a flat interface. Since the surface is flat, any point of a finite-size source will be imaged to a point with the same x -coordinate. Thus $\Delta x = 0$ and $\Phi_x = 0$. One only needs to consider Φ_z . A generalized Fermat's principle states that *an image will be formed if the phase Φ_z is stationary*, $d\Phi_z/dk_z = 0$. The lens equation for a single interface is

$$u = \sigma v \quad (1)$$

with a material constant

$$\sigma = -dk_{rz}/dk_z. \quad (2)$$

This constant σ should be positive and independent of the incident angle for a focus without aberration. Thus the following rule for the wave vector refraction at the interface must be obeyed

$$k_{rz} = \kappa - \sigma k_z. \quad (3)$$

Here κ is the integration constant which is also an intrinsic property of the ENGRM. Since in the vacuum $k_z^2 + k_x^2 = k_0^2 = \omega_0^2/c^2$, the equi-frequency surface (EFS) of the medium is

$$\sigma^{-2}(\kappa - k_{rz})^2 + k_x^2 = \omega_0^2/c^2. \quad (4)$$

Note that this elliptic dispersion exists only at the operating frequency ω_0 [19]. In the neighborhood of this frequency $\omega \sim \omega_0$, $(\kappa - k_{rz})^2/n_z^2 + k_x^2/n_x^2 = \omega^2/c^2$ with $\tilde{\sigma} \equiv n_z/n_x \sim \sigma$. The deduction of Eq. (3) from an elliptic EFS requires *negative group refraction*

$$(\mathbf{k}_r - \kappa \hat{\mathbf{z}}) \cdot \nabla_{\mathbf{k}_r} \omega < 0 \quad (5)$$

together with the causality condition $\partial\omega/\partial k_{rz} > 0$ that the energy must flow away from the interface which is illustrated in Fig. 2. The ray vector [20] which represents the direction of group velocity in a medium with elliptic EFS is $\mathbf{s} = (-\tilde{\sigma} \sin \alpha \hat{\mathbf{x}} + \cos \alpha \hat{\mathbf{z}})/n_x \tilde{\sigma}$ while $\mathbf{k}_r - \kappa \hat{\mathbf{z}} = n_x (\sin \alpha \hat{\mathbf{x}} - \tilde{\sigma} \cos \alpha \hat{\mathbf{z}})$ with $\sin \alpha = n_x^{-1} \sin \theta$ and θ the incident angle in the vacuum.

The Snell's law for wave vector loses its meaning in this anisotropic medium. However there is a law for group refraction, which is $\tan \beta = -\tilde{\sigma} \tan \alpha = -\tilde{\sigma} (n_x^2 - \sin^2 \theta)^{-1/2} \sin \theta$. At the operating frequency ω_0 of the flat lens, $n_x = 1$, $\tilde{\sigma}(\omega_0) = \sigma$, the group refraction law is simply

$$\tan \beta = -\sigma \tan \theta. \quad (6)$$

Thus $-\sigma$ can be regarded as the effective refractive index. Note that this refraction law is very general and is valid

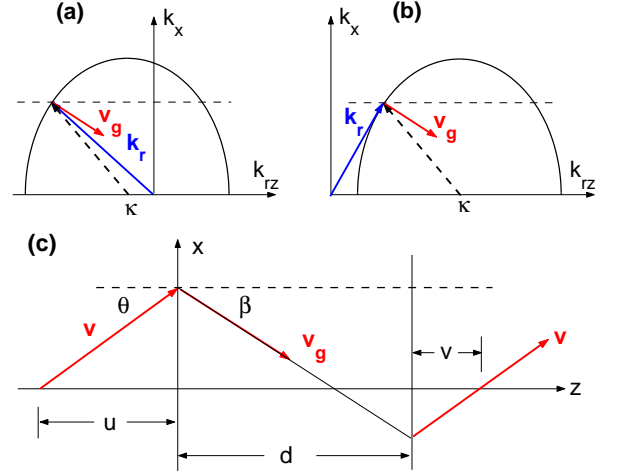


FIG. 2: Group velocity for an ENGRM with elliptic EFS and $(\mathbf{k}_r - \kappa \hat{\mathbf{z}}) \cdot \nabla_{\mathbf{k}_r} \omega < 0$ and (a) negative or (b) positive wave vector refraction. The dashed arrow is $\mathbf{k}_r - \kappa \hat{\mathbf{z}}$. (c) Ray diagram of the group velocity for imaging by an ENGRM flat lens with $u + v = \sigma d$.

for any σ as defined by Eq. (2). The proof is the following, $\tan \beta = \frac{\partial\omega}{\partial k_{rx}} / \frac{\partial\omega}{\partial k_{rz}} = \frac{dk_{rz}}{dk_x} \frac{\partial\omega}{\partial k_x} / \frac{\partial\omega}{\partial k_z} = -\sigma \tan \theta$. Here we used $k_{rx} = k_x$.

The space inside the medium can be considered to be “optically stretched” in the z -direction by a factor of σ^{-1} . The waves inside the medium are represented by $\psi(\mathbf{r}') = \exp(ik_x x - ik_z z' + i\kappa' z')$ with $z' = \sigma z$ and $\kappa' = \kappa/\sigma$. Thus in the case that $\kappa \neq 0$, the waves at this frequency will experience a periodicity in the z -direction with length scale $2\pi/|\kappa|$ since the waves are modulated by $\exp(i\kappa z)$. This periodicity is the effective periodicity and may not be the actual physical periodicity such as the lattice spacing of a PhC.

We now consider the imaging of an ENGRM slab with thickness d as shown in Fig. 1(b). The first surface is at the origin and the second at $z = d$. A point source is placed at $z = -u$. We consider another point outside the ENGRM slab at $z = d + v$. If the value of v satisfies the following lens equation

$$u + v = \sigma d, \quad (7)$$

the phase difference $\Phi_z = k_z(u + v) + k_{rz}d = \kappa d$ is stationary and an image will be formed without aberration. Note that for an ordinary thin curved lens with focal length f , the lens equation is $u^{-1} + v^{-1} = f^{-1}$. With given value of σ and slab thickness d , the distance between the object and the image outside the slab is fixed, $u + v + d = (1 + \sigma)d$. Once the location of the object is fixed, the position of the image is also fixed, no matter where the slab is placed!

We remark that a flat slab can focus with *negative* as well as with *positive* wave vector refraction. The necessary condition for flat lens imaging is *negative group refraction*. In general, there is not much meaning of Snell's law for wave vectors for anisotropic media. Only the re-

fraction law for the direction of group velocity Eq. (6) is meaningful and does correspond to ray diagrams. The Veselago-Pendry lens is a special case of our flat lens with $\sigma = 1$, $\kappa = 0$ and is the only case that the ray diagram is applicable for the wave vectors.

The lensmaker's formula Eq. (1) or (7) only provides a necessary condition for imaging. An additional constraint is required for the formation of a "perfect" image, viz. the surface reflection coefficient r should vanish, $r = 0$, for far field and should diverge, $r \rightarrow \infty$, for near field. These set the conditions for a perfect flat lens without optical axis. The requirement of no reflection $r = 0$ is not essential for a slab to focus far field. The principal conditions for the flat lens to focus light are that Eq. (3) and $|r| \ll 1$ should be satisfied for all or at least a large range of incident angles. The presence of reflection will make the image dim and may give rise to multiple images. The indefinite indices medium [21] can have an elliptic dispersion relation, but in general will not satisfy the flat lens imaging conditions.

The field inside the ENGRM flat lens can also be described by a partial differential equation $[\sigma^{-2}(\partial_x + \partial_z)^2 + \partial_x^2 + (\omega/c)^2]\Psi = 0$. The medium can be regarded as a distorted space with the metric $ds^2 = dx^2 + \sigma^2 dz^2$. Thus there is an analogy with gravitational lensing where refraction occurs due to the warping of space caused by general relativistic effects, such as in the vicinity of a massive object. It is worth noting that general relativistic effects are observable due to optical refraction.

In the rest of the paper, we will focus on S -polarized electromagnetic waves with the electric field in the y -direction. In general, the magnetic permeability μ of the ENGRM should be a tensor, and its relationship to the other material parameters σ and κ can be deduced. Here we assume that effective indices ϵ and μ can be used to describe the medium of interest. Due to its symmetry, the ellipsoid can always be transformed to its principal axes [2]. For the S -polarized waves, the H field is in the xz -plane, only μ_x and μ_z will enter our discussion. Furthermore, μ_x plays a more active role than μ_z since the surface reflection coefficient is $r = (\mu_x k_z - k_{rz})/(\mu_x k_z + k_{rz})$. Thus to achieve perfect imaging for far field, the effective permeability of ENGRM should be

$$\mu_x = \kappa/k_0 \cos \theta - \sigma. \quad (8)$$

Only in the case $\kappa = 0$ that $\mu_x = -\sigma$ is isotropic while for $\kappa \neq 0$, μ_x has to be anisotropic and diverges at $k_x = k_0$. For $\kappa \neq 0$, any finite μ_x at $k_x = k_0$ results in reduced transmission. Notice that in PhCs including metamaterials, the effective μ_x should be anisotropic in general.

To see how the propagating waves are focused, we consider a S -polarized point source $-(i/4)H_0^{(1)}(k_0|\mathbf{r} + u\hat{\mathbf{z}}|)$ which is centered at $z = -u$ while the two surfaces of the ENGRM slab are at $z = 0$ and $z = d$. If μ_x takes the form given by Eq. (8), there will be no reflection for propagating waves and the transmission coefficient through the slab is $T = \exp(ik_{rz}d)$. The transmitted far

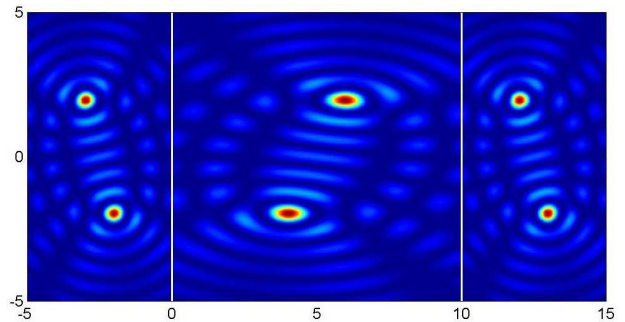


FIG. 3: Field intensity of two sources ($J_0(k_0 r)$) imaged by an ENGRM flat lens with $\sigma = 0.5$, $\kappa = 0$, and thickness $d = 10$. The two white lines indicate the surfaces of the lens. We set $\mu_x = -0.5$ for the ENGRM for perfect transmission.

field is

$$E_{\text{far}}^t(\mathbf{r}) = -ie^{i\kappa d} \int_0^{\pi/2} \frac{d\theta}{2\pi} e^{ik_z[z+u-(1+\sigma)d]} \cos(k_x x). \quad (9)$$

Note that $k_z = k_0 \cos \theta$ and $k_x = k_0 \sin \theta$. The image outside the slab is located at $z = (1 + \sigma)d - u$. One can see that except for a global phase $\exp(i\kappa d)$, the far field of the image is exactly that of the source. The far field inside the slab is

$$E_{\text{far}}^{\text{in}}(\mathbf{r}) = -ie^{i\kappa z} \int_0^{\pi/2} \frac{d\theta}{2\pi} e^{-ik_z(\sigma z - u)} \cos(k_x x) \quad (10)$$

for $0 \leq z \leq d$. Another perfect image is formed inside the slab at $z = u/\sigma$. The first surface acts as a mirror with an extra phase $\exp(i\kappa z)$. The space inside the ENGRM slab is optically stretched by a factor of σ^{-1} . A flat lens imaging is shown in Fig. 3.

Evanescent waves and sub-wavelength imaging For evanescent waves $k_x > k_0$, the complex extrapolation of Eq. (4) gives

$$k_{rz} = \kappa + i\sigma q \quad (11)$$

with $q \equiv (k_x^2 - k_0^2)^{1/2}$. The transmission coefficient through the flat lens is $T = (1 - r^2) \exp(ik_{rz}d) / [1 - r^2 \exp(2ik_{rz}d)]$ with $r = [(\mu_x - \sigma)q + i\kappa] / [(\mu_x + \sigma)q - i\kappa]$. In order to amplify evanescent waves, a singularity must exist in T to compensate to certain extent the decay of evanescent waves in the vacuum $\exp[-q(u + v)]$. In the case of single-interface resonance [9, 24], $r \rightarrow \infty$, $T \exp[-q(u + v)] = \exp(i\kappa d)$, all the evanescent waves will be amplified only if

$$\mu_x = \mu_x^0 \equiv -\sigma + i\kappa/q. \quad (12)$$

The images both inside and outside have the same sub-wavelength features of the source. If μ_x couldn't take the above form, sub-wavelength imaging is still possible. At the so-called overall resonance condition [24], $1 - r^2 \exp(2ik_{rz}d) = 0$, thus $r = \pm \exp(-ik_{rz}d)$, one gets

$$\mu_x = \mu_x^\pm \equiv (-\sigma + i\kappa/q) \tanh^{\mp 1}(\sigma q - i\kappa)d/2. \quad (13)$$

For $\kappa \neq 0$, μ_x^0 and μ_x^\pm are all complex with negative real parts. One notices that $\mu_x^+(q)$ is flatter than $\mu_x^-(q)$ as functions of q . In terms of effective indices, the existence of surface modes $\omega_0(k_x)$ requires that $\Re\mu_x$ be negative for S -polarization. To amplify evanescent waves, the $\omega_0(k_x)$ curve must be very flat [24]. This is equivalent to say that the curve $\mu_x^+(q)$ should be flat so that the contribution of evanescent waves are constructive for certain window of q . The closer μ_x is to $\mu_x^+(q)$, the more sub-wavelength features the images will have. Note that for large κd , the evanescent waves are located in the vicinity of the interfaces for constant μ_x .

Realization in real materials We note that no known natural material is found to have negative dispersion. Negative group refraction can be achieved in periodic or quasi-periodic media with nonzero κ [22]. For most media, Eq. (8) and (12) are unlikely to be fulfilled, thus a perfect flat lens is unattainable. Realization using real materials is discussed next.

Ordinary material may not have the EFS described by Eq. (4) for all k_x . For an uniaxial crystal, since the group refraction is positive, thus $k_{rz} = \kappa - \sigma k_z$ with $\kappa = 0$ and $\sigma < 0$. There will be no focus though negative refraction for certain incident angles can be easily achieved [23]. Instead a virtual image will be formed satisfying the same lens equation. However, a PhC could have *both* an elliptic EFS and negative group refraction for certain windows of k_x at certain frequency. Here we use some general features of PhCs to explain the imaging mechanism. To this end, we consider the first band of a square lattice PhC of unit lattice spacing. For small k_x along the ΓM direction, the dispersion can be approximated elliptically as $k_{rz} \simeq \kappa - \sigma_0 k_z$ with appropriate constants κ and σ_0 (see the dashed line in Fig. 4). At $\omega_0 = \omega_u$, the upper limit of all-angle negative refraction (AANR) in the first band [13], $\kappa = \sqrt{2\pi} - k_0(1 - \sigma_0)$. Since for AANR with ω_0 away from ω_u , σ_0 will be smaller, we only concentrate here on the discussion for $\omega_0 = \omega_u$. To enhance the transmission, the slab thickness can be selected to satisfy the Fabry-Perot resonance condition $(\kappa - \sigma_0\omega/c)d = 0 \pmod{2\pi}$. The slab is on resonance only for $k_x \rightarrow 0$. For large k_x , $k_{rz} \simeq \sqrt{2\pi} - \sigma_0^{-1/2}k_z$ due to the C_{4v} symmetry of the EFS. A desired large transmission would require μ_x to diverge. Thus the image location is bounded $\sigma_0 \leq (u+v)/d \leq \sigma_0^{-1/2}$ and the Fourier components of the object with $k_x \rightarrow k_0$ will be partially lost. This leads to a so-called *self-collimation effect* for small σ_0 . Far field images both inside and outside the slab with reasonably good quality will be formed. However, the image inside the PhC is stretched and modulated due to the partial transmission besides the Bloch wave modulation. Even with the removal of Bloch wave modulation, the image inside a PhC will be visible only for large thickness. For evanescent waves at $\omega = \omega_u$ with $k_x \rightarrow k_0$, one has $\Re\mu_x^0 = -\sigma_0^{-1/2}$ and $\Im\mu_x^0 \rightarrow \infty$ while for $k_x \gg k_0$, $\mu_x^\pm(k_x) \simeq \mu_x^0(k_x) \rightarrow -\sigma_0^{-1}$. To have substantial sub-wavelength feature of the image, the real part of μ_x

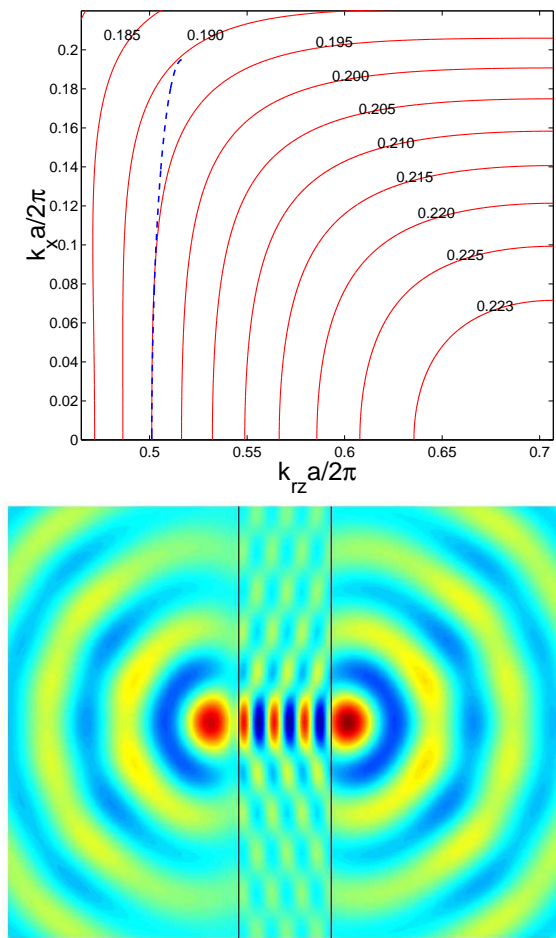


FIG. 4: (a) EFS of the TE modes of a square lattice PhC calculated using plane wave expansion. (b) Far-field H_z of a point source across an ENGRM slab with dispersion relation $k_{rz} = \kappa - \sigma k_z$ with $\kappa = 3.2465$ and $\sigma = 0.08$ which approximates the actual EFS of the PhC (dashed line in the upper panel). The permittivity $\epsilon_x = 2.2$ is used. Note the modulated field inside the homogeneous ENGRM. Due to impedance mismatch, the images are not “perfect” unlike Fig. 3.

must take large negative value for small σ_0 . An example is shown in Fig. 4, which is very similar to Fig. 5 in Ref. [13]. The image is confined in the vicinity of the second surface of the PhC slab due to a small value of σ_0 .

In this paper, we have discussed the group refraction of an anisotropic medium characterized by two materials parameters σ and κ . When σ is a positive constant, the anisotropic medium is an ENGRM and a flat slab of such medium can be used as a focal lens without optical axis and leading to images free of aberration. Our theory of flat lens imaging is a generalization of the Vesalago-Pendry perfect lens and beyond Silin’s formula. The theory is valid for both real and virtual images. This flat lens theory leads to a clear understanding of negative group refraction and flat lens imaging in electromagnetism [13, 14], acoustics [25], and electron waves.

Numerical simulations of homogeneous ENGRMs and of PhCs were carried out supporting our theory.

The lack of optical axis for the flat lens has very broad applications and confers important advantages in optics. Clearly there are no aperture restrictions. There are two characteristics that might be viewed as limitations. The lensmaker's formula clearly dictates upper bounds to $u, v < \sigma d$ for real image formation. The other limitation is that magnification is always unity. For any medium the

lens properties σ, κ , and also the working frequency ω_0 can be obtained by inspection of the EFS. To have high quality image, σ should be constant and close to unity. The present theory can be used to design tailor-made flat lenses. Extension of our theory to three-dimensions is straightforward.

Work supported by the National Science Foundation and the Air Force Research Laboratories, Hanscom, MA.

-
- [1] B. Mahon, *The man who changed everything: The life of James Clerk Maxwell*, John Wiley & Sons 2004.
- [2] M. Born and E. Wolf, *Principles of Optics*, 7th ed., Cambridge University Press (2003).
- [3] E. W. Marchland, *Gradient Index Optics*, Academic Press, New York (1978).
- [4] P. B. Wilkinson, T. M. Fromhold, R. P. Taylor, and A. P. Micolich, Phys. Rev. Lett. **86**, 5466 (2001).
- [5] D. R. Smith, J. J. Mock, A. F. Starr, and D. Schurig, Phys. Rev. E **71**, 036609 (2005).
- [6] S. A. Tretyakov, in *Negative Refraction: Revisiting Electromagnetics from Microwave to Optics*, EPFL Latsis Symposium, Lausanne, Switzerland, 2005, pp.30-35.
- [7] V. G. Veselago, Sov. Phys. Usp. **10**, 509 (1968).
- [8] R. A. Silin, Opt. Spectrosc. **44**, 109 (1978).
- [9] J. B. Pendry, Phys. Rev. Lett. **85**, 3966 (2000).
- [10] R. A. Shelby, D. R. Smith, and S. Shultz, Science **292**, 77 (2001).
- [11] E. Cubukcu, K. Aydin, E. Ozbay, S. Foteinopoulou, and C. M. Soukoulis, Nature (London) **423**, 604 (2003).
- [12] P. V. Parimi, W. T. Lu, P. Vodo, J. Sokoloff, J. S. Derov, and S. Sridhar, Phys. Rev. Lett. **92**, 127401 (2004).
- [13] C. Luo, S. G. Johnson, and J. D. Joannopoulos, Phys. Rev. B **65**, 201104(R) (2002).
- [14] P. V. Parimi, W. T. Lu, P. Vodo, and S. Sridhar, Nature (London) **426**, 404 (2003).
- [15] J. T. Shen and P. M. Platzman, Appl. Phys. Lett. **80**, 3286 (2002).
- [16] W. T. Lu and S. Sridhar, Microwave Opt. Tech. Lett. **39**, 282 (2003).
- [17] N. Fang, H. Lee, C. Sun, and X. Zhang, Science **308**, 534 (2005).
- [18] D. O. S. Melville and R. J. Blaikie, Opt. Express **13**, 2127 (2005).
- [19] Note that the Veselago-Pendry lens also operates at a single frequency for which $n = \epsilon = \mu = -1$.
- [20] L. Landau and I.M. Lifshitz, *Electrodynamics of continuous media*, 2nd Ed. (Elsevier 1984).
- [21] D.R. Smith and D. Schurig, Phys. Rev. Lett. **90**, 077405 (2003).
- [22] For a PhC with negative group refraction, κ is always nonzero. For example for the second band, $\kappa \sim 2\pi/a$ instead of $\kappa \sim 0$.
- [23] Y. Zhang, B. Fluegel, and A. Mascarenhas, Phys. Rev. Lett. **91**, 157404 (2003).
- [24] C. Luo, S. G. Johnson, J. D. Joannopoulos, and J. B. Pendry, Phys. Rev. B **68**, 045115 (2003).
- [25] X. Zhang and Z. Liu, Appl. Phys. Lett. **85**, 341 (2004).